Journal of Reproduction and Development, Vol. 65, No 5, 2019

—Original Article—

Studying the variations in differently expressed serum proteins of Hainan black goat during the breeding cycle using isobaric tags for relative and absolute quantitation (iTRAQ) technology

Rui HUA[1)], Lu ZHOU[1)], Haiwen ZHANG[1, 2)], Hui YANG[1)], Wenchuan PENG[1)] and Kebang WU[1, 2)]

[1)]*Key Laboratory of Tropical Animal Breeding and Epidemic Disease Research of Hainan Province, Hainan University, Hainan 570228, People's Republic of China*

[2)]*Laboratory of Tropical Animal Breeding, Reproduction and Nutrition, Hainan University, Hainan 570228, People's Republic of China*

Abstract. The Hainan black goat is a high-quality local goat breed in Hainan Province of China. It is resistant to high temperatures, humidity, and disease. Although the meat of this breed is tender and delicious, its reproductive performance and milk yield are low. In this study, isobaric tags for relative and absolute quantitation (iTRAQ) technology was used to analyze the differentially expressed proteins in the serum of female Hainan black goats during the reproductive cycle (empty pregnant, estrus, gestation, and lactation). The pathway enrichment analysis results showed that most of the differentially expressed proteins between each period belonged to the complement and coagulation cascades. Analysis of the differential protein expression and function revealed seven proteins that were directly associated with reproduction, namely pre-SAA21, ANTXR2, vWF, SFRP3, β4GalT1, pre-IGFBP2 and Ran. This study revealed the changing patterns of differentially expressed proteins in the reproductive cycle of the Hainan black goat. pre-SAA21, ANTXR2, vWF, SFRP3, β4GalT1, pre-IGFBP2, and Ran were identified as candidate proteins for mediating the physiological state of Hainan black goats and regulating their fertility. This study elucidated the changes in expression levels of differentially expressed proteins during the reproductive cycle of Hainan black goats and also provides details about its breeding pattern.

Key words: Cell proliferation, Hainan black goat, Isobaric tags for relative and absolute quantitation (iTRAQ) technology, Proteomics, Reproductive cycle

(**J. Reprod. Dev. 65:** 413–421, 2019)

The Hainan black goat, also known as the Hainan East goat, is a local goat breed that has long been bred in the unique natural ecological environment of Hainan Province of China. It has the advantages of being resistant to high temperature, humidity, and various diseases, with tender and delicious meat without uncomfortable flavor, making it a popular choice among consumers [1]. Currently, research on black goats is mainly focused on improving their production performance and meat quality by changing the feed nutrient composition. Adding n-3 polyunsaturated fatty acid (PUFA) rich oil to the feed can significantly increase the number of preovulatory follicles and ovulation rate, and also mediate the improvement of kidding rate [2]. Similarly, melatonin can increase the oocyte viability in juvenile goat, as it can increase the number and quality of embryos [3].

Proteomics studies assess the protein characteristics on a large scale, including the expression level, posttranslational modifications, and protein-protein interactions. This emerging technology has improved our understanding of the dynamic changes in the life of proteins. The isobaric tags for relative and absolute quantitation (iTRAQ) technology can simultaneously use isotope-based reagents to label eight polypeptide samples. The labeled polypeptide samples are mixed in equal volumes and analyzed by liquid chromatography separation and tandem mass spectrometry (LC-MS/MS), and the first and second stage mass spectrum information of each peptide are obtained. In the first-order MS, the same peptides from different samples show the same mass-to-charge ratio. In the second-order MS, the mass-to-charge ratios of peptide fragment ions and the signal intensities of the eight iTRAQ reporter ions indicate the peptide sequence information, and the relative expression of the peptide in different samples. The identified proteins and their differential expression in each sample can be identified through bioinformatics analysis [4, 5].

Since its development, iTRAQ technology has been widely used in quantitative proteomics research because of its unique advantages. Using the serum of locoweed-poisoned and healthy rabbits for quantitative protein analysis by iTRAQ, Zhang *et al*. [6] have found that locoweed may damage the rabbit's nerve cells to reduce its immunity. Wei *et al*. [7] ethave used iTRAQ technology to measure the protein expression in the serum of Wistar rats exposed to different concentrations of sodium fluoride, and found that differentially

Received: September 5, 2018
Accepted: June 20, 2019
Advanced Epub: July 14, 2019

Correspondence: K Wu (e-mail: wukebang66@sina.com)

expressed proteins mainly belonged to complement and coagulation cascades, inflammatory responses, and complement activation pathways, indicating that inflammation and immune response may play a key role in the mechanism of fluorosis. Ren *et al*. [8] have used iTRAQ technology to study the changes in protein expression in sheep liver caused by overgrazing. They found that the reduction in animal growth caused by overgrazing was associated with changes in the liver proteome, especially in proteins involved in nitrogen compound metabolism and immunity.

Hainan black goats usually attain sexual maturity at 4–6 months of age, and first breed at 7–8 months of age. They normally produce a single kid per year and sometimes three kids in two years. The reproductive performance and milk yield are relatively low. It is well-known that proteins in serum change with the shift of age, physiological state, and nutritional conditions, which directly reflect the pathological and physiological condition of an individual. In addition, serum collection is convenient and causes less stress on the goats. It avoids killing the experimental goats, which will be used for continuous observation and sampling. To date, research on the reproduction of Hainan black goats has not been reported. In this study, we used iTRAQ proteomics technology to analyze the protein expression in the Hainan black goat serum during the anestrous, estrus, gestation, and lactation periods. Our aim was to explore the changing patterns of differentially expressed proteins during the reproductive cycle of Hainan black goats, and to provide basic data for their breeding.

Materials and Methods

Ethical statement for animal care

All procedures were approved by the animal care and use committee of Hainan University (HU 20170912). All efforts were made to minimize the suffering of animals during the sampling process and sacrifice.

Sample collection

In this study, we divided the breeding cycle of the ewes into four stages: anestrous period (from the end of lactation to the next estrus), 1–2 days of estrus period (follicular phase), 3–4 months of gestation period, and a month of lactation period. Twelve healthy one-and-a-half-year-old Hainan black goats, well-developed in Hainan black goat Breeding Base were selected. Each period contained three individuals as the biological repeats. The blood samples were collected from the jugular veins of experimental animal, and allowed to stand for 2 h without violent shocks. After the blood coagulated and serum separated out, the samples were centrifuged at 4390 × *g* for 10 min, the supernatant was removed, marked, and placed in –80°C refrigerator for later use.

Experiment process

In this study, the extracted serum proteins were assessed for quality, and then pretreated with alkylation, enzymolysis, and salt removal. Peptides were labeled with iTRAQ tags and separated by liquid chromatography, the end of separation was connected to the mass spectrometer. The raw data of the mass spectrometry was converted, searched in the database, and assessed for quality. The qualified samples were further analyzed using bioinformatics (Fig. 1).

Protein extraction and quality control

Proteins were extracted using the Protominer kit (BioRad, Hercules, CA, USA), and protein concentration and sample integrity were assessed by the Bradford assay (Amresco, Burlington, NC, USA), and polyacrylamide gel electrophoresis (BBI, Shanghai, China).

Sample marking and loading

To 100 μg of protein solution, 2.5 μg of Trypsin enzyme (Promega, Madison, WI, USA) was added, and incubated at 37ºC for 4 h; then, Trypsin enzyme was supplemented once again, and incubated at 37ºC for 8 h. The enzymatic peptides were desalted and vacuum-dried using Strata X column (Phenomenex, Los Angeles, CA, USA). Fifty microliters of isopropanol (Fisher Scientific, Waltham, MA, USA) was added, the samples were vortexed, and then centrifuged at 4000 r/min for 5 min. The peptide samples were dissolved in 0.5 M TEAB (SCIEX, Framingham, MA, USA), and added to the corresponding iTRAQ tagging reagents (SCIEX); different iTRAQ tags were used for different samples (SCIEX). The samples were

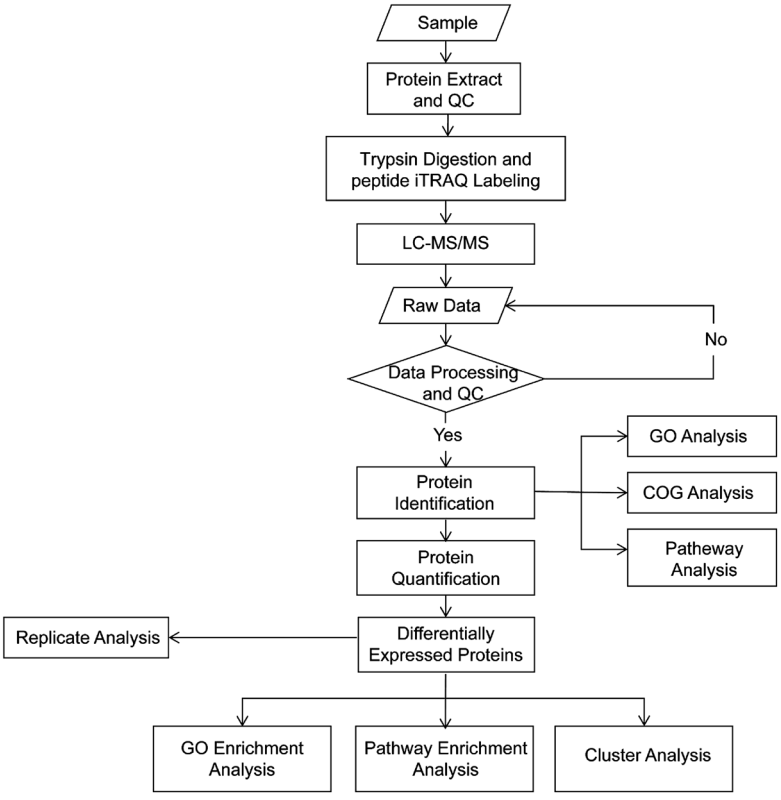

Fig. 1. Experimental flowchart.

allowed to stand for 2 h at room temperature. The separation was performed by LC-20AD nanoliter liquid chromatograph (Shimadzu, Kyoto, Japan), and the Triple TOF 5600 mass spectrometer (SCIEX) was attached to the end.

Mass spectrometry detection

The liquid-phase separated peptides were subjected to mass spectrometry, with parameters set as follows: the ion source (SCIEX) spray voltage was 2300 V, and nitrogen pressure was 30 psi. The spray gas was 15, and spray interface was at 150ºC. The high-sensitivity mode was used for scanning. The cumulative time of the first-level mass spectrum scan was 250 msec, and the scanning mass range was 350–1500 Da. According to the ionic strength in the first-order spectrum from high to low, select the top 30 with the intensity exceeding 150 cp for fragmentation and scan the secondary information. The screening criteria were as follows: the m/z range was 350–1250 Da; the number of charges was 2–5; dynamic exclusion of parent ions was set such that in half of the peak time (about 12 sec) and the fragmentation of the same parent ion was not more than 2 times. The cumulative scan time of the secondary mass spectrometer was 100 msec. For the iTRAQ type of data acquisition, the fragmentation energy selection was adjusted according to the iTRAQ reagent, and the ion transmission efficiency of the second quadrupole Q2 at 100 Da was 100%. The product time was 100 msec.

Bioinformatics analysis

The original MS data was converted into MGF format by the Proteo Wizard tool msConvert software (http://proteowizard.sourceforge.net/). The MGF file was compared with Mascot software (http://www.matrixscience.com/) and protein sequence database to obtain the final protein identification result.

iTRAQ data was quantified using IQuant software [9]. The 1% FDR (false discovery rate) filtration was initially performed at the spectrum/peptide level to obtain significant spectra and peptides lists. Based on the parsimony principle [10], peptides were used for protein assembly to generate a series of protein groups. In order to control the false positive rate of protein detection, the protein level was again filtered with FDR 1%, the strategy used was Picked protein FDR [11].

The GO (Gene Ontology) functional annotation was performed by Blast2go software, and all identified proteins were compared with the corresponding non-redundant (NR) protein database (ftp://ftp.ncbi.nlm.nih.gov/genomes/Capra_hircus/protein/protein.fa.gz) to obtain the corresponding GO function. In the GO enrichment analysis of differentially expressed proteins, the hypergeometric test was used to find significantly enriched GO items, by comparing the differentially expressed protein to all the proteins identified. Pathway enrichment analysis of differentially expressed proteins was similar to GO enrichment analysis.

Results

iTRAQ identification

Samples that passed the quality control test were analyzed by LC-MS/MS, and a total of 1,011,548 secondary spectrograms were generated. A total of 5745 peptides and 1213 proteins were identified under the "1% FDR" filtration standard (Table 1 and Supplementary files 1–3: online only). Three repeat groups identified 722, 746, and 825 proteins, and the number of proteins identified in all three groups was 442 (Fig. 2).

In this study, the four stages of the reproductive cycle were compared with each other to identify differentially expressed serum proteins. The distribution of coefficient of variance (CV) in the three replicate experiments (Fig. 3) was found to be concentrated in the range of 0 to 30%, and the cumulative number of proteins below 30% of CV distribution was 74%, 83%, 77%, 79%, 78%, and 86%, indicating good repeatability of the data.

Proteins that showed significant differential expression were screened using the values of fold change > 1.2 and Q-value < 0.05. The number of differentially expressed proteins was highest in the anestrous and gestation periods, with 63 upregulated and 138 downregulated proteins, and the lowest number of differentially expressed proteins in the anestrous period compared with the lactation period was a total of 106 proteins (46 upregulated and 60 downregulated). Compared with the estrus period, 101, 93, and 66 proteins were upregulated, and 69, 79, and 75 proteins were downregulated during the gestation, lactation, and anestrous periods, respectively. The number of proteins that were up- and downregulated in the lactation period compared to the gestation period was 58 and 101 proteins, respectively (Table 2 and Supplementary files 4–9: online only).

Bioinformatics analysis

The GO analysis (Fig. 4) mainly includes three parts: cellular component, molecular function, and biological process. The cell component was divided into 17 groups, mainly into cell, cell part, organelle, and organelle part; the molecular function was divided into 17 groups, mainly related to the binding and catalytic activity; the biological process was divided into 26 groups, mainly related to single-organism process, cellular process, biological regulation, regulation of biological process, multicellular organismal process, response to stimulus, and metabolic process.

All the identified proteins were compared with the COG database to obtain the corresponding COG annotation results. The COG annotation results (Fig. 5) showed that the functions of the proteins concentrated mainly on posttranslational modification, protein turnover, chaperones, and general function prediction.

Pathway enrichment analysis of differentially expressed proteins (Fig. 6) showed that the pathway annotated with the maximum number of differentially expressed proteins was the complement and coagulation cascade, between the anestrous and estrus period, the anestrous and gestation period, the gestation and estrus period, the lactation and estrus period, and the lactation and gestation period. Comparing the anestrous with lactation period revealed that most differentially expressed proteins were concentrated in the metabolic pathway. The pathways annotated with the largest Rich Factor (RF) were the Fanconi anemia pathway (anestrous and estrus period), adipocytokine signaling (anestrous and gestation period), arachidonic acid metabolism (anestrous and lactation period), p53 signaling (gestation and estrus period, lactation and gestation period), and prolactin signaling pathway (lactation and estrus period). These results suggested that the protein expression in the serum of Hainan black goats at different stages of reproduction was mainly associated

Table 1. Overview of protein identification

Sample name	Total spectra	Spectra	Unique spectra	Peptide	Unique peptide	Protein
Capra_hircus_1	338816	22654	20776	3831	3563	722
Capra_hircus_2	335614	23580	21762	3984	3760	746
Capra_hircus_3	337118	27958	24944	4316	3983	825
Total	1011548	74192	67482	5745	5465	1213

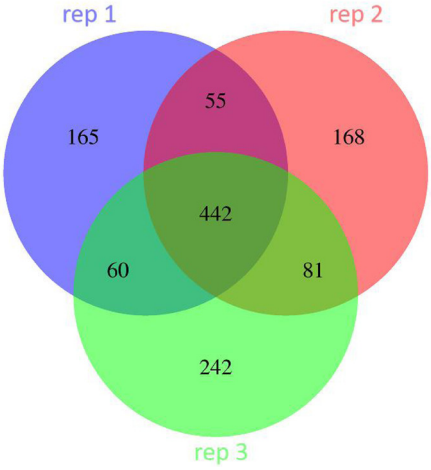

Fig. 2. Venn diagram of protein quantitation. Three different colors represent three biological repeats, blue represents repeat 1, red represents repeat 2, and green represents repeat 3.

with immunity and nutrient metabolism.

Analysis of differential protein expression and function revealed seven proteins that were directly associated with reproduction. These proteins were identified as pre-SAA21, ANTXR2, vWF, SFRP3, β4GalT1, pre-IGFBP2 and Ran. SFRP3 increased significantly during the estrus period compared with the anestrous period. Compared with the estrus period, there were three differentially expressed proteins during the gestation period: pre-SAA21 (upregulated), ANTXR2 (downregulated), and Ran (downregulated). The expression of pre-IGFBP2 was significantly decreased during the anestrous period compared with the lactation period. The expression of β4GalT1 was higher in the estrus period than the anestrous period, and lower during the lactation period than the gestation period. The expression of vWF was significantly downregulated during gestation compared with the estrus period and upregulated during the lactation period compared with the gestation period (see Table 3 for a detailed list of the seven proteins).

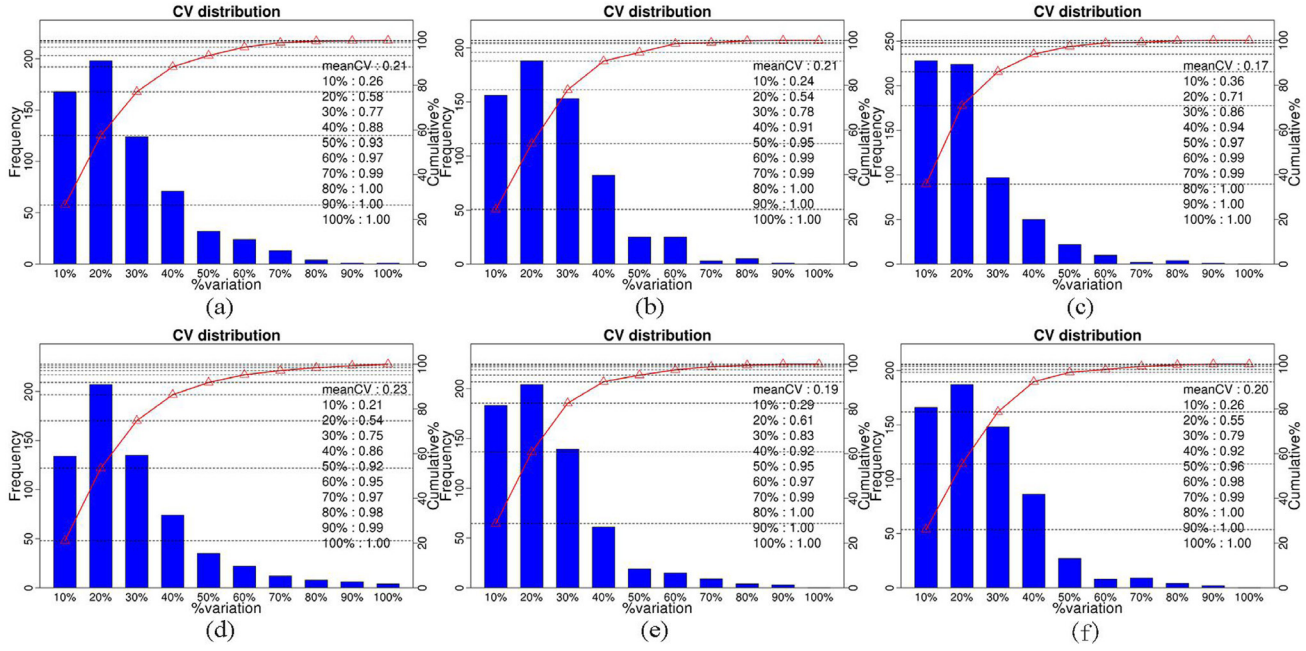

Fig. 3. Distribution of coefficient of variance (CV) in the repeated experiments. The X axis represents the CV distribution range, the Y axis represents the number of proteins in the corresponding CV range, and the right side of the figure is the number of accumulated proteins in each CV range. a~f represent the repetition test CV distribution for the four stages of the reproductive cycle: a. anestrous period-*vs.*-estrus period; b. anestrous period-*vs.*-gestation period; c. anestrous period-*vs.*-lactation period; d. gestation period-*vs.*-estrus period; e. lactation period-*vs.*-estrus period; f. lactation period-*vs.*-gestation period.

Table 2. List of differently expressed proteins

Compare group	Upregulated	Downregulated	All-regulated
anestrous period-*vs.*-estrus period	66	75	141
anestrous period-*vs.*-gestation period	63	138	201
anestrous period-*vs.*-lactation period	46	60	106
gestation period-*vs.*-estrus period	101	69	170
lactation period-*vs.*-estrus period	93	79	172
lactation period-*vs.*-gestation period	58	101	159

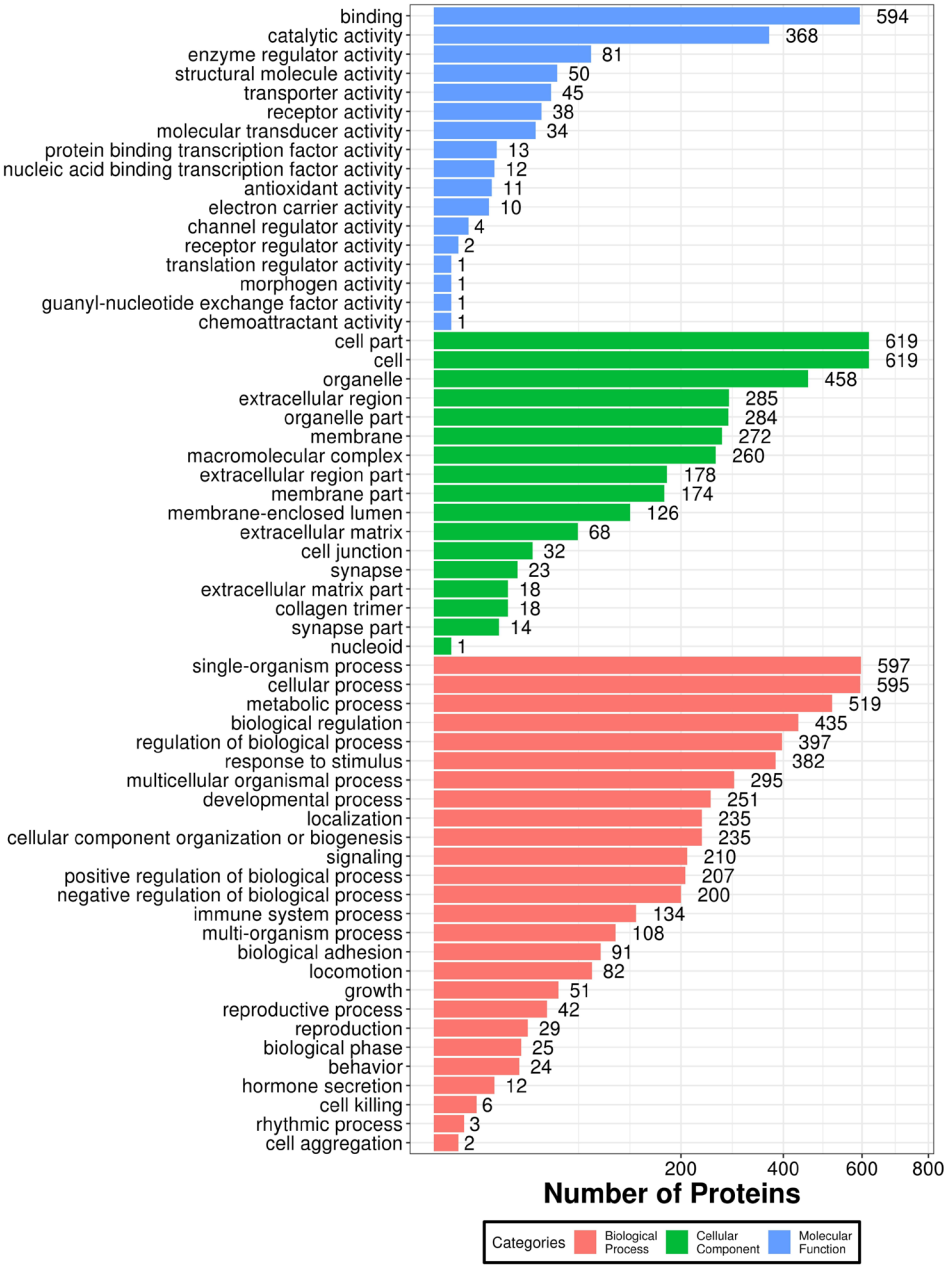

Fig. 4. Gene oncology (GO) annotation bar chart. The histograms are GO annotations for the three GO classifications, the Y axis represents the GO entry, and the X axis represents the number of proteins annotated with the corresponding GO entry. Different colors in the figure represent different GO classifications, with red representing a biological process, green representing a cellular component, and blue representing a molecular function.

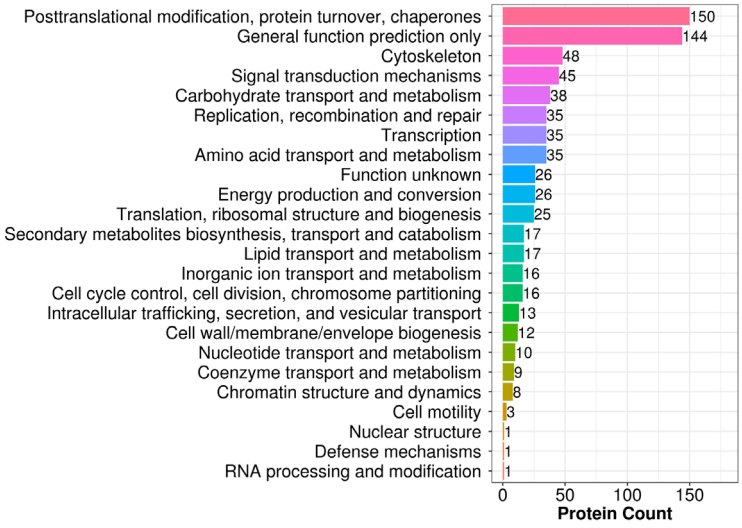

Fig. 5. COG annotation bar chart. The Y axis represents the COG entry and the X axis represents the number of proteins annotated with the corresponding COG entry.

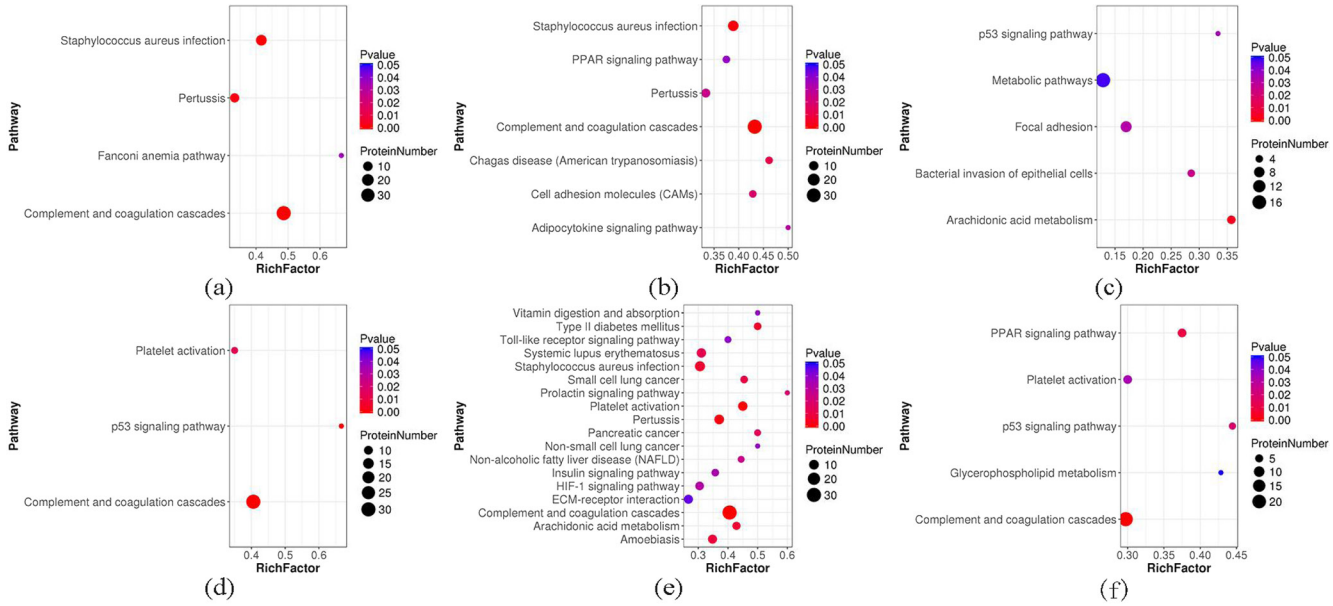

Fig. 6. Significantly enriched pathway chart. The Rich Factor (RF) for the X axis represents the number of differently expressed proteins annotated to the pathway divided by the total identified proteins annotated to the pathway; and the higher the value, the greater the proportion of differently expressed proteins that are annotated to the pathway. Sizes of the dot in the figure represent the number of differently expressed proteins annotated to the pathway. a~f represent the KEGG pathway significant enrichment analysis of the differently expressed proteins during the four reproductive stages: a. anestrous period-*vs.*-estrus period; b. anestrous period-*vs.*-gestation period; c. empty pregnant phase-*vs.*-lactation period; d. gestation period-*vs.*-estrus period; e. lactation period-*vs.*-estrus period; f. lactation period-*vs.*-gestation period.

Discussion

In this study we used iTRAQ proteomics technology to analyze the protein expression in the breeding cycle of Hainan black goats. The data showed that the pathway enriched for maximum RF in estrus ewes compared with empty pregnant ewes was the Fanconi anemia (FA) pathway. The function of the FA pathway is mainly to repair the covalent cross-linking between dsDNA in the DNA damage response (DDR) [12]. In addition, FA proteins are involved in selective autophagy of pathogens and subcellular particles, regulating inflammation and genotoxic stress [13]. This implies that the defensive abilities against external environment stimulation and exogenous

Table 3. List of protein molecular functions annotated with reproduction stage

Description	Differential expression stage	Mean ratio	Ratio	Q value
PREDICTED: serum amyloid A21 precursor	gestation period-*vs.*-estrus period ↑	1.76	1.929|1.376|1.972	0.004|0.121|0.001
PREDICTED: anthrax toxin receptor 2	gestation period-*vs.*-estrus period ↓	0.65	0.570|0.657|0.713	0.160|0.013|0.063
PREDICTED: von Willebrand factor	gestation period-*vs.*-estrus period ↓	0.74	0.784|0.872|0.572	0.001|0.001|0.001
	lactation period-*vs.*-gestation period ↑	1.28	1.265|1.043|1.547	0.001|0.071|0.001
PREDICTED: secreted frizzled-related protein 3	anestrous period-*vs.*-estrus period ↓	0.72	0.670|0.826|0.653	0.027|0.016|0.009
PREDICTED: beta-1,4-galactosyltransferase 1	lactation period-*vs.*-gestation period ↓	0.52	0.595|-|0.441	0.065|-|0.002
	anestrous period-*vs.*-estrus period ↓	0.56	0.579|-|0.542	0.117|-|0.004
PREDICTED: insulin-like growth factor-binding protein 2 precursor	anestrous period-*vs.*-lactation period ↓	0.84	0.934|0.647|0.947	0.284|0.001|0.819
PREDICTED: GTP-binding nuclear protein Ran	gestation period-*vs.*-estrus period ↓	0.48	0.505|-|0.462	0.016|-|0.001

substances should be improved during the estrus period. The pathway enriched for maximum RF in gestation period compared with estrus period, and lactation period compared with gestation period was the p53 signaling pathway, with RF of 0.67 and 0.44, respectively. This suggested that changes in protein expression may be associated with regulating cell proliferation, embryonic development, and preparing for childbirth. It has been reported that maintaining p53 pathway protein level plays an important role in embryonic normal development and embryonic stress response; and abnormal activation of p53 signaling can lead to embryonic lethality [14, 15]. Deng *et al*. [16] have found that the interaction of p53 and sestrins proteins can coordinate AMPK and TORC1 signaling to determines parturition timing. KEGG annotation of the pre-IGFBP2 protein revealed that it participates in the p53 pathway, cellular senescence, and transcriptional misregulation in cancer. IGFBP generally regulates cell proliferation, differentiation, and apoptosis by interacting with insulin-like growth factor (IGF) or by acting independently [17–19]. Srividya *et al*. [20] have found that IGFBP3 plays an important role in the development of preantral follicles to mature follicles. In this study, pre-IGFBP2 showed a lower serum level during the anestrous period than during the lactation period. It may participate in the p53 signaling pathway, which induces self-repairing of the body by mediating cell proliferation and apoptosis. Furthermore, posttranslational processing may play a role in generating IGFBP2 for regulating follicle development and ovulation during the next estrus.

The pathways annotated with the highest number of differentially expressed proteins in each stage of the reproductive cycle are the complement and coagulation cascade, 36 (anestrous *vs.* estrus period), 30 (gestation *vs.* estrus period), 22 (lactation *vs.* gestation period) respectively. Complement and coagulation play an important role in limiting the innate response towards bleeding and infection at the injury site [21]. Liu *et al*. [22] demonstrated that the glutathione S-transferase and serpin families are involved in glutathione metabolism, TGF-beta signaling, and complement and coagulation cascades, which can reduce oxidative stress and inflammatory response, and improve immunity. A large number of proteins in this study, belonging to the complement and coagulation cascades, were involved in enhancing the resistance of ewes to inflammatory and infectious diseases. Three of the seven screened proteins, namely, β4GalT1, pre-SAA21, and vWF were immune-related. Glycosylation is an important protein modification process. β4GalT is an enzyme, specifically responsible for catalyzing galactosylation, and plays an important role in the cell-matrix interaction, nervous system development, immunity and inflammation, and tumor development [23–25]. Zhao *et al*. [24] have found that β4GalT1 affects the galactosylation of carbohydrates, and regulates the biosynthetic process of selectin ligands to mediate inflammatory cell adhesion and migration. The GO annotation and KEGG analysis results in this study indicated that β4GalT1 was mainly involved in the biological processes of galactose metabolism and lactose biosynthesis, acute inflammatory response, and in angiogenesis associated with wound healing. The level of β4GalT1 in the estrus period was higher than that in the anestrous period. It may regulate physiological processes, such as estrus and ovulation, via regulating the biosynthesis and metabolism of carbohydrates in the Hainan black goats. It may also regulate the immune system to mediate the adhesion and migration of inflammatory cells. However, to elucidate the detailed mechanisms, further research is required. The secretion levels of β4GalT1 in the serum samples of lactating ewes decreased significantly compared with gestating ewes, possibly owing to the preparation of subsequent lactation. A large amount of β4GalT1 is involved in the biosynthesis of galactose, which is one of the main components of milk. Serum amyloid A (SAA) is an acute phase reactive protein that usually binds to high-density lipoproteins. Ather *et al*. [26] have suggested that SAA may serve as a candidate biomarker for the development of inflammation. In this study, iTRAQ technology revealed that the secretory level of pre-SAA21 (SAA21 is a subtype of SAA) increased significantly during the gestation period compared with the estrus period. GO and KEGG analysis showed that pre-SAA21 mainly participated in three pathways of protein processing, associated with the endoplasmic reticulum, phagosome formation, and antigen processing and presentation. As ewes enter the gestation period, their appetite increases, and the metabolism becomes more vigorous. The reason for the increased secretion of pre-SAA21 may be to stimulate the immune response and improve the body's immunity and antiviral ability. vWF is a polysaccharide protein secreted by endothelial cells and megakaryocytes that plays an important role in hemostasis. It can combine with collagen fibers to promote blood platelet adhesion to the injured part; it can also combine with factor VIII to protect it from hydrolysis by proteases [27, 28]. A study [29] has shown that the expression level of vWF is

associated with bacterial translocation, inflammation, and procoagulant imbalance. The serum level of vWF decreased in ewes during gestation compared with the estrus period, indicating that pregnant ewes had poor resistance to bacteria, viruses, and other foreign substances; thus bacterial translocation was more likely to occur. Preventive measures, such as adding anti-inflammatory drugs to feed should be taken to improve the disease-resistance ability of the pregnant ewes. After the kids were born, the ewes entering the lactation period experienced a tremendous change in physiology and metabolism, as well as in stress, which affected the health to a certain extent. Significantly higher serum vWF levels observed during lactation than those during the gestation period might be due to the fact that the body needs to improve its ability to resist invasion of foreign substances and maintain internal environmental stability, thereby preventing the occurrence of mastitis.

The functions of ANTXR2 and SFRP3 are related to cell proliferation. A previous study [30] has shown that ANTXR2 regulates directional mitosis by interacting with both RhoA and F-actin proteins, and directional mitosis plays an important role in embryogenesis and organogenesis [31]. Li *et al*. [32] have also revealed that directional mitosis contributes to trabecular morphogenesis and regional specification. The GO and KEGG analysis of ANTXR2 in this study showed that ANTXR2 is mainly involved in the PI3K-Akt signaling pathway, ECM-receptor interaction, and the protein digestion and absorption pathway. PI3K-Akt signaling regulates not only proliferation, differentiation, and apoptosis, but also glucose transport and other cellular functions. ANTXR2 secretion decreased in the goat serum during the gestation period compared with the estrus period. It may be that ANTXR2 plays a crucial role in early embryonic development, organogenesis, histogenesis and other physiological processes by mediating directional mitosis.

SFRP can inhibit the activity of Wnt protein through competitive binding with the frizzled receptor (FZD) on the cell surface, thereby inhibiting abnormal cell division and proliferation [33]. The main biological function of Wnt proteins is to regulating the cell proliferation, apoptosis, adhesion, and migration [34–37]. A previous study [35] has shown that SFRP1 can inhibit cell proliferation and migration, and promote apoptosis of colorectal cancer cells. In this study, we revealed that the level of secreted SFRP3 was upregulated at the estrus stage compared with that at the gestation stage; and GO annotation showed that the molecular functions of SFRP3 were PDZ domain binding, Wnt-activated receptor activity, and Wnt-protein binding. SFRP3 may mediate the Wnt signaling pathway to regulate proliferation of granulosa cells during follicular development. The proliferation, differentiation, and hormone secretion function of granulosa cells in the ovary are closely associated with the development and maturation of oocytes.

The GTP-binding nuclear protein, also known as Ras-associated nuclear protein (Ran), is a member of the Ras superfamily. Ran participates as a "molecular switch" in the cell cycle by binding to GTP or GDP, and plays an important role in nucleocytoplasmic transport, spindle assembly, and nuclear envelope formation [38, 39]. Nagai *et al*. [40] have found that downregulation of Ran results in a decrease in the cytoplasmic and nuclear accumulation of imported proteins, thereby accelerating cell aging in normal cells. In this study, the metabolism of ewes strengthened after entering the gestation period. In addition, it is necessary to provide various nutrients for the growth and development of the fetus. The ewe's demand for carbohydrates, proteins, and other nutrients is greatly increased. According to the GO and KEGG analysis, Ran is mainly involved in RNA transport and ribosome biosynthesis. Analyzing the reason behind the observed decrease in the gestation period compared to the estrus period suggested that a high level of Ran may participate in the biosynthesis of ribosomes to regulate protein synthesis and metabolism. This implies that we should pay attention to the comprehensive and reasonable nutrition in the feeding and management of pregnant ewes, and if necessary, appropriate supplements should be added.

In summary, we analyzed the expression profile of the serum proteome of Hainan black goats during different breeding periods (anestrous, estrum, gestation, and lactation periods) using iTRAQ technology. We detected several changes in immunity, inflammation, cell proliferation, apoptosis, adhesion, migration, and nutrient metabolism during the different breeding periods, which might be associated with the low fertility. pre-SAA21, ANTXR2, vWF, SFRP3, β4GalT1, pre-IGFBP2, and Ran were identified as candidate proteins that mediate the physiological state of the Hainan black goat. However, the possible reason for the small change observed in protein expression might be due to the presence of feedback regulation mechanisms in the secretion system of functional proteins *in vivo*. Upon reaching a certain threshold in the serum, a corresponding mechanism may exist to regulate the further secretion of protein to avoid damage caused by overexpression. The functions of these differentially expressed proteins remain largely unknown, and further research is required to clarify their roles in the goat breeding cycle, which may help to improve the fertility of Hainan black goats.

Acknowledgements

This study was financially supported by the key technology research and integration application of large-scale healthy breeding of Hainan black goats (Grant No. ZDKJ2016017) and research and application of meat key gene screening and molecular assistant breeding of the special wild boar in Hainan Province (Grant No. ZDYF2017059).

References

1. **Hu J, Zhao W, Niu L, Wang L, Li L, Zhang H, Zhong T.** Gene organization and characterization of the complete mitochondrial genome of Hainan black goat (Capra hircus). *Mitochondrial DNA A DNA Mapp Seq Anal* 2016; **27**: 1656–1657. [Medline]
2. **Mahla AS, Chaudhari RK, Verma AK, Singh AK, Singh SK, Singh G, Sarkar M, Dutta N, Kumar H, Krishnaswamy N.** Effect of dietary supplementation of omega-3 polyunsaturated fatty acid (PUFA) rich fish oil on reproductive performance of the goat (Capra hircus). *Theriogenology* 2017; **99**: 79–89. [Medline] [CrossRef]
3. **Soto-Heras S, Roura M, Catalá MG, Menéndez-Blanco I, Izquierdo D, Fouladi-Nashta AA, Paramio MT.** Beneficial effects of melatonin on in vitro embryo production from juvenile goat oocytes. *Reprod Fertil Dev* 2018; **30**: 253–261. [Medline] [CrossRef]
4. **Brewis IA, Brennan P.** Proteomics technologies for the global identification and quantification of proteins. *Adv Protein Chem Struct Biol* 2010; **80**: 1–44. [Medline] [CrossRef]
5. **Dayon L, Sanchez JC.** Relative protein quantification by MS/MS using the tandem mass tag technology. *Methods Mol Biol* 2012; **893**: 115–127. [Medline] [CrossRef]
6. **Zhang JH, Li Y, Song XB, Ji XH, Sun HN, Wang H, Fu SB, Zhao LJ, Sun DJ.** Differential expression of serum proteins in rats subchronically exposed to arsenic identified by iTRAQ-based proteomic technology-14-3-3 ζ protein to serve as a potential biomarker. *Toxicol Res (Camb)* 2016; **5**: 651–659. [Medline] [CrossRef]
7. **Wei Y, Zeng B, Zhang H, Chen C, Wu Y, Wang N, Wu Y, Shen L.** iTRAQ-based

proteomics analysis of serum proteins in Wistar rats treated with sodium fluoride: insight into the potential mechanism and candidate biomarkers of fluorosis. *Int J Mol Sci* 2016; **17**: 17. [Medline] [CrossRef]

8. **Ren W, Hou X, Wang Y, Badgery W, Li X, Ding Y, Guo H, Wu Z, Hu N, Kong L, Chang C, Jiang C, Zhang J.** Overgrazing induces alterations in the hepatic proteome of sheep (*Ovis aries*): an iTRAQ-based quantitative proteomic analysis. *Proteome Sci* 2017; **15**: 2. [Medline] [CrossRef]
9. **Wen B, Zhou R, Feng Q, Wang Q, Wang J, Liu S.** IQuant: an automated pipeline for quantitative proteomics based upon isobaric tags. *Proteomics* 2014; **14**: 2280–2285. [Medline] [CrossRef]
10. **Brosch M, Yu L, Hubbard T, Choudhary J.** Accurate and sensitive peptide identification with Mascot Percolator. *J Proteome Res* 2009; **8**: 3176–3181. [Medline] [CrossRef]
11. **Savitski MM, Wilhelm M, Hahne H, Kuster B, Bantscheff M.** A scalable approach for protein false discovery rate estimation in large proteomic data sets. *Mol Cell Proteomics* 2015; **14**: 2394–2404. [Medline] [CrossRef]
12. **Siddiqui MQ, Rajpurohit YS, Thapa PS, Maurya GK, Banerjee K, Khan MA, Panda P, Hasan SK, Gadewal N, Misra HS, Varma AK.** Studies of protein-protein interactions in Fanconi anemia pathway to unravel the DNA interstrand crosslink repair mechanism. *Int J Biol Macromol* 2017; **104**(Pt A): 1338–1344. [Medline] [CrossRef]
13. **Sumpter R Jr, Levine B.** Emerging functions of the Fanconi anemia pathway at a glance. *J Cell Sci* 2017; **130**: 2657–2662. [Medline] [CrossRef]
14. **Ishimura A, Terashima M, Tange S, Suzuki T.** Jmjd5 functions as a regulator of p53 signaling during mouse embryogenesis. *Cell Tissue Res* 2016; **363**: 723–733. [Medline] [CrossRef]
15. **El Husseini N, Schlisser AE, Hales BF.** Editor's highlight: hydroxyurea exposure activates the P53 signaling pathway in murine organogenesis-stage embryos. *Toxicol Sci* 2016; **152**: 297–308. [Medline] [CrossRef]
16. **Deng W, Cha J, Yuan J, Haraguchi H, Bartos A, Leishman E, Viollet B, Bradshaw HB, Hirota Y, Dey SK.** p53 coordinates decidual sestrin 2/AMPK/mTORC1 signaling to govern parturition timing. *J Clin Invest* 2016; **126**: 2941–2954. [Medline] [CrossRef]
17. **Key TJ, Appleby PN, Reeves GK, Roddam AW, Breast TEH. Endogenous Hormones and Breast Cancer Collaborative Group.** Insulin-like growth factor 1 (IGF1), IGF binding protein 3 (IGFBP3), and breast cancer risk: pooled individual data analysis of 17 prospective studies. *Lancet Oncol* 2010; **11**: 530–542. [Medline] [CrossRef]
18. **Wang XL, Li YN, Chen L, Hou ZQ.** Insulin-like growth factor binding protein 2 regulates cell proliferation and migration in the adjuvant arthritis synovial cells through ERK signaling pathway. *Int J Clin Exp Pathol* 2017; **10**: 3219–3226.
19. **Zhang XL, Li HH, Cao YP, Peng F, Li JP.** Insulin-like growth factor binding protein 3 inhibits inflammatory response and promotes apoptosis in fibroblast-like synoviocytes of osteoarthritis. *Int J Clin Exp Pathol* 2017; **10**: 3024–3032.
20. **Srividya D, Praveen Chakravarthi V, Kona S, Siva Kumar A, Brahmaiah KV, Rao VH.** Expression of kit ligand and insulin-like growth factor binding protein 3 during in vivo or in vitro development of ovarian follicles in sheep. *Reprod Domest Anim* 2017; **52**: 661–671. [Medline] [CrossRef]
21. **Conway EM.** Complement-coagulation connections. *Blood Coagul Fibrinolysis* 2018; **29**: 243–251. [Medline]
22. **Liu R, Liu J, Zhao G, Li W, Zheng M, Wang J, Li Q, Cui H, Wen J.** Relevance of the intestinal health-related pathways to broiler residual feed intake revealed by duodenal transcriptome profiling. *Poult Sci* 2019; **98**: 1102–1110. [Medline]
23. **Shen A, Yan J, Ding F, Gu X, Zhu D, Gu J.** Overexpression of beta-1,4-galactosyltransferase I in rat Schwann cells promotes the growth of co-cultured dorsal root ganglia. *Neurosci Lett* 2003; **342**: 159–162. [Medline] [CrossRef]
24. **Zhao J, Gao Y, Cheng C, Yan M, Wang J.** Upregulation of β-1,4-galactosyltransferase I in rat spinal cord with experimental autoimmune encephalomyelitis. *J Mol Neurosci* 2013; **49**: 437–445. [Medline] [CrossRef]
25. **Vanhooren V, Vandenbroucke RE, Dewaele S, Van Hamme E, Haigh JJ, Hochepied T, Libert C.** Mice overexpressing β-1,4-Galactosyltransferase I are resistant to TNF-induced inflammation and DSS-induced colitis. *PLoS One* 2013; **8**: e79883. [Medline] [CrossRef]
26. **Ather JL, Poynter ME.** Serum amyloid A3 is required for normal weight and immunometabolic function in mice. *PLoS One* 2018; **13**: e0192352. [Medline] [CrossRef]
27. **Zhang C, Kelkar A, Nasirikenari M, Lau JTY, Sveinsson M, Sharma UC, Pokharel S, Neelamegham S.** The physical spacing between the von Willebrand factor D'D3 and A1 domains regulates platelet adhesion in vitro and in vivo. *J Thromb Haemost* 2018; **16**: 571–582. [Medline] [CrossRef]
28. **Jacobi PM, Kanaji S, Jakab D, Gehrand AL, Johnsen JM, Haberichter SL.** von Willebrand factor propeptide to antigen ratio identifies platelet activation and reduced von Willebrand factor survival phenotype in mice. *J Thromb Haemost* 2018; **16**: 546–554. [Medline] [CrossRef]
29. **Mandorfer M, Schwabl P, Paternostro R, Pomej K, Bauer D, Thaler J, Ay C, Quehenberger P, Fritzer-Szekeres M, Peck-Radosavljevic M, Trauner M, Reiberger T, Ferlitsch A, Lab VHH. Vienna Hepatic Hemodynamic Lab.** Von Willebrand factor indicates bacterial translocation, inflammation, and procoagulant imbalance and predicts complications independently of portal hypertension severity. *Aliment Pharmacol Ther* 2018; **47**: 980–988. [Medline] [CrossRef]
30. **Castanon I, Abrami L, Holtzer L, Heisenberg CP, van der Goot FG, González-Gaitán M.** Anthrax toxin receptor 2a controls mitotic spindle positioning. *Nat Cell Biol* 2013; **15**: 28–39. [Medline] [CrossRef]
31. **Li Y, Li A, Junge J, Bronner M.** Planar cell polarity signaling coordinates oriented cell division and cell rearrangement in clonally expanding growth plate cartilage. *eLife* 2017; **6**: 6. [Medline] [CrossRef]
32. **Li J, Miao L, Shieh D, Spiotto E, Li J, Zhou B, Paul A, Schwartz RJ, Firulli AB, Singer HA, Huang G, Wu M.** Single-cell lineage tracing reveals that oriented cell division contributes to trabecular morphogenesis and regional specification. *Cell Reports* 2016; **15**: 158–170. [Medline] [CrossRef]
33. **Hsieh M, Mulders SM, Friis RR, Dharmarajan A, Richards JS.** Expression and localization of secreted frizzled-related protein-4 in the rodent ovary: evidence for selective up-regulation in luteinized granulosa cells. *Endocrinology* 2003; **144**: 4597–4606. [Medline] [CrossRef]
34. **Wang BM, Li N.** Effect of the Wnt/β-catenin signaling pathway on apoptosis, migration, and invasion of transplanted hepatocellular carcinoma cells after transcatheter arterial chemoembolization in rats. *J Cell Biochem* 2018; **119**: 4050–4060. [Medline] [CrossRef]
35. **Wang Z, Li R, He Y, Huang S.** Effects of secreted frizzled-related protein 1 on proliferation, migration, invasion, and apoptosis of colorectal cancer cells. *Cancer Cell Int* 2018; **18**: 48. [Medline] [CrossRef]
36. **Heinosalo T, Gabriel M, Kallio L, Adhikari P, Huhtinen K, Laajala TD, Kaikkonen E, Mehmood A, Suvitie P, Kujari H, Aittokallio T, Perheentupa A, Poutanen M.** Secreted frizzled-related protein 2 (SFRP2) expression promotes lesion proliferation via canonical WNT signaling and indicates lesion borders in extraovarian endometriosis. *Hum Reprod* 2018; **33**: 817–831. [Medline] [CrossRef]
37. **Deshmukh A, Arfuso F, Newsholme P, Dharmarajan A.** Regulation of cancer stem cell metabolism by secreted frizzled-related protein 4 (sFRP4). *Cancers (Basel)* 2018; **10**: 10. [Medline] [CrossRef]
38. **Nagai M, Yoneda Y.** Small GTPase Ran and Ran-binding proteins. *Biomol Concepts* 2012; **3**: 307–318. [Medline] [CrossRef]
39. **Zhang MS, Arnaoutov A, Dasso M.** RanBP1 governs spindle assembly by defining mitotic Ran-GTP production. *Dev Cell* 2014; **31**: 393–404. [Medline] [CrossRef]
40. **Nagai M, Yoneda Y.** Downregulation of the small GTPase ras-related nuclear protein accelerates cellular ageing. *Biochim Biophys Acta* 2013; **1830**: 2813–2819. [Medline] [CrossRef]